Computation of Deformable Interface Two-Phase Flows: A Semi-Lagrangian Finite Element Approach

Rafael A. Vidal[1], Daniel B. V. Santos[1], Prashant Valluri[2], Gustavo R. Anjos*[1]

[1]*COPPE — Department of Mechanical Engineering, Universidade Federal do Rio de Janeiro - Rio de Janeiro, Brazil – gustavo.rabello@coppe.ufrj.br*
[2]*IMT — Chemical Eng, School of Engineering, University of Edinburgh - Edinburgh, United Kingdom*

Abstract. This work aims at presenting a computational approach to study two-phase flows and the coalescence phenomenon using direct numerical simulation. The flows are modeled by the incompressible Navier-Stokes equations, which are approximated by the Finite Element Method. The Galerkin formulation is used to discretize the Navier-Stokes equations in the spatial domain and the semi-Lagrangian method is used to discretize the material derivative backward in time. In order to satisfy the Ladyzhenskaya–Babuška–Brezzi condition, high-order pair of elements are used, with pressure and velocity fields being calculated on different sets of the unstructured mesh nodes. The interface is modeled by an uncoupled adaptive moving mesh, where interface nodes are tracked in a Lagrangian fashion and moved with the velocity solution of the motion equations. The interface tension is computed using the interface curvature and the gradient of a Heaviside function, and added in the momentum equations as a volume force. In order to stabilize the simulation, a smooth transition between fluid properties is defined on the interface region. Several benchmark tests have been carried out to validate the proposed approach, and the obtained results have demonstrated agreement with analytical solutions and results reported in the literature. A coalescence modeling is also proposed considering geometric parameters and results show interesting dynamics.

Keywords: Two-phase flows, coalescence, Finite Element Method, semi-Lagrangian, unstructured mesh.

1 Introduction

Multiphase flows are present in a variety of natural phenomena and industrial applications. Atmosphere, ocean waves, blood circulation, and various other flows in our daily lives are characterized by the presence of more than one phase. In the industry, the current situation is no different. Cooling systems using phase-changing fluids are employed in a wide range of applications, from electronic components to nuclear power plants. The combustion of liquid fuels, also essential for a significant portion of human activities, is usually preceded by atomization into droplets to form an air-fuel mixture with a larger contact surface. Oil extraction involves the simultaneous flow of oil, gas, water, and occasional solid particles. Therefore, as declared by Tryggvason et al. [1], it would not be an exaggeration to state that virtually all industrial fluid applications today involve flows with multiple phases. From this statement, one can deduce that the development of methods for studying and simulating multiphase flows – and, in particular, two-phase flows – is highly relevant not only for understanding and predicting natural phenomena but also for improving industrial processes.

An important distinction among two-phase flow simulation methodologies consists in the particle system interpretation, which can be classically classified between the Eulerian and the Lagrangian approaches. More recently, the semi-Lagrangian approach, which combines the characteristics of Eulerian and Lagrangian interpretations, rised in popularity. In this method, although the scalar field is defined with respect to static spatial points, particle movement is considered to determine a virtual position of these points at the previous time instant, at each time step. Although widely used today, the mathematical concept of the semi-Lagrangian method dates back to the mid-20th century. In 1959, the semi-Lagrangian method was first described by Wiin-Nielsen [2], and in 1963, Sawyer [3] synthesized it in a very similar way to the one used in this work. In both cases, the application of the semi-Lagrangian method focused on meteorology, for weather forecasting through the simulation of atmospheric flows – field in which it achieved notable relevance due to two of its main characteristics: unconditional stability

and the possibility of using high time steps. Although consolidated in meteorology, the use of the semi-Lagrangian method for the direct numerical simulation of the Navier-Stokes equations was not as frequent and grew gradually. In 1990, Maday et al. [4] applied first, second, and third-order semi-Lagrangian methods to simulate flows modeled by incompressible Navier-Stokes equations. In 1994, Boukir et al. [5] compared a first-order and a second-order semi-Lagrangian method to evaluate a steady flow of a vortex in a cavity and a transient problem of natural convection. In 2000, Phillips and Phillips [6] validated the application of the semi-Lagrangian method to simulate flows around a cylinder with Reynolds number varying between 1 and 50. Over the years, the complexity of the simulated flows has increased. In 2015, Celledoni et al. [7] proposed a class of higher-order semi-Lagrangian methods using Spectral Element Methods for spatial discretization and exponential integrators for temporal evolution of the simulation, for flows with high Reynolds numbers. In 2021, Wilde et al. [8] presented a model based on high-order semi-Lagrangian methods and the lattice Boltzmann equation, applied to the analysis of turbulence in three-dimensional compressible flows. In 2022, Anjos et al. [9] proposed an approach based on the second-order semi-Lagrangian method, in conjunction with the Finite Element Method and the Arbitrary Lagrangian-Eulerian formulation, for the simulation of two-dimensional axisymmetric flows.

Based on the application of the semi-Lagrangian method for a wide variety of simulations of varying degrees of complexity in recent times, this work aims to present the use of this approach in an interface-tracking methodology for the simulation of two-phase flows.

2 Methodology

In the proposed methodology, the two-phase flows are modeled by the incompressible Navier-Stokes equations, as shown in (1) and (2), where the last two terms respectively represent gravity and interfacial tension forces. An one-fluid approach is employed, whereby the domain occupied by the two phases is described by a single set of equations. The two-phase phenomenon is obtained by associating different density and viscosity values to each region of the domain, as well as including the interfacial tension force as a body force in the last equation.

$$\nabla \cdot \mathbf{v} = 0 \tag{1}$$

$$\rho \left[\frac{\partial \mathbf{v}}{\partial t} + \mathbf{v} \cdot \nabla \mathbf{v} \right] = -\nabla p + \frac{1}{Re} \nabla \cdot [\mu \left(\nabla \mathbf{v} + \nabla \mathbf{v}^T \right)] + \frac{1}{Fr^2} \rho \, \mathbf{g} + \frac{1}{We} \mathbf{f} \tag{2}$$

These equations are approximated by the Finite Element Method, and the Galerkin method is employed to discretize its continuous variables in the spatial domain. An unstructured static mesh is defined throughout the spatial domain, and the Ladyzhenskaya–Babuška–Brezzi stability condition is verified to ensure the formulation's stability. For the two-dimensional approach, mini and quadratic triangular elements were selected to compose the mesh, while for the three-dimensional approach, the choice was for the mini element due to its lower associated computational cost.

After the application of the Galerkin method, spatially discrete equations are obtained. For the numerical simulation of the problem, it is necessary to discretize the material derivative to obtain discrete equations in both space and time. In this work, such discretization is performed using the semi-Lagrangian method. Let $\mathbf{x_i}$ be the position of a mesh node, and $\mathbf{x_d}$ be the virtual starting position at time n of a fluid particle that reached position $\mathbf{x_i}$ at time $n+1$. Let $\mathbf{v_i^{n+1}}$ be the fluid velocity at point $\mathbf{x_i}$ at time $n+1$, and $\mathbf{v_d^n}$ be the fluid velocity at point $\mathbf{x_d}$ at time n. The semi-Lagrangian method approximates the material derivative of velocity as shown in (3). To calculate $\mathbf{v_d^n}$, it is necessary to first calculate the position $\mathbf{x_d^n}$ using an estimate of the previous position of the mesh nodes, given by (4). When the point $\mathbf{x_d}$ remains inside the mesh, its velocity $\mathbf{v_d}$ is interpolated from the velocities of the nodes of the element which contains it. When the point $\mathbf{x_d}$ exits the domain, it is determined which boundary it surpassed, and $\mathbf{v_d}$ is set as the velocity corresponding to that boundary condition.

$$\frac{D\mathbf{v_i}}{Dt} \approx \frac{\mathbf{v_i^{n+1}} - \mathbf{v_d^n}}{\Delta t} \tag{3}$$

$$\mathbf{x_d^n} = \mathbf{x_i^{n+1}} - \mathbf{v_i^{n+1}} \, \Delta t \tag{4}$$

An interface-tracking model is applied, where the interface is explicitly defined by a sequential set of points. These points are independent of the static mesh that discretizes the domain and are moved over it as the iterations progress. To assign density and viscosity properties to the nodes of the static mesh, a region Ω_{in} interior to the set of interface points and a region Ω_{out} exterior to Ω_{in} are defined. The properties of each fluid are associated with the nodes belonging to each of these regions. To provide a smooth transition of properties at the interfacial region and thus avoid numerical instabilities, a smoothed Heaviside function $H_\epsilon(\phi)$, proposed by Sussman and Smereka

[10], was employed to generate density and viscosity fields. It is shown in (5), where ϵ is half of the interface thickness and ϕ is the distance from a point to the interface.

$$H_\epsilon(\phi) = \begin{cases} 0 & \text{se } \phi < -\epsilon \\ \frac{1}{2}\left[1 + \frac{\phi}{\epsilon} + \frac{1}{\pi}\, sen(\frac{\pi\,\phi}{\epsilon})\right] & \text{se } -\epsilon \leq \phi \leq \epsilon \\ 1 & \text{se } \phi > \epsilon \end{cases} \tag{5}$$

Thus, the density and viscosity of each node of the static mesh are calculated according to (6) and (7), respectively.

$$\rho(\phi) = \rho_{in}\, H_\epsilon(\phi) + \rho_{out}\, (1 - H_\epsilon(\phi)) \tag{6}$$

$$\mu(\phi) = \mu_{in}\, H_\epsilon(\phi) + \mu_{out}\, (1 - H_\epsilon(\phi)) \tag{7}$$

For modeling the interfacial tension, the curvature is calculated at each interface point, and the calculated curvature is distributed to the static mesh. Then, with the curvature κ and the smoothed Heaviside function H_ϵ for each node of the static mesh, the interfacial tension formulation of Unverdi and Tryggvason [11] is extended as shown in (8).

$$\mathbf{f} = \sigma\, \kappa\, \delta\, \mathbf{n} = -\sigma\, \kappa\, \nabla H \tag{8}$$

The temporal and spatial discretization of the problem transforms it into a linear system, and the temporal evolution of the flow is obtained by solving this system consecutively. At the end of each iteration, the points that make up the interface mesh are moved with the velocity imposed by the static mesh. To avoid clustering of the interface points over time, the velocity of each interface point is decomposed into a normal and a tangential components, and only the normal component is considered for its movement.

The interface remeshing algorithm implemented in this methodology defines a minimum acceptable distance d_{min} – given by half of the average length of the edges of the static mesh elements – and a maximum acceptable distance d_{max} – given by twice the average length of the edges of the static mesh elements – between each pair of adjacent interface points. After moving the interface in each iteration of the simulation, the distance between each pair of adjacent points is calculated. For two consecutive interface points separated by a distance d, the following procedure is executed: if $d < d_{min}$, the last point is removed; if $d > d_{max}$, a point is added at the geometric center between them. This ensures a spacing between interface points that is sufficiently homogeneous and compatible with the static mesh that discretizes the domain.

Furthermore, to evaluate the applicability of the methodology for describing flows with topological changes, a purely geometric model is proposed to describe the coalescence phenomenon. When two bubbles approach each other, a boundary layer forms between their interfaces, which, to be adequately described in the current methodology, would require the presence of some static mesh elements in that region. In the case where the distance between the bubbles is less than one element, for example, it can be said that the bubbles are so close that the methodology described so far would no longer be sufficient to describe the phenomena occurring in that region of the flow. Therefore, this methodology proposes that when the minimum distance between the interfaces of two bubbles becomes smaller than d_{min}, these interfaces merge, resulting in a larger bubble. The points of a bubble that are at a distance less than $2\, d_{min}$ from the other bubble are excluded, and the remaining points form a single interface. This coalescence model has already been implemented for two-dimensional flows, and its extension to three dimensions is programmed for the next steps of this work.

3 Results

This section exposes the results of the simulations that were carried out, with the aim of validating the described methodology. Two test cases are shown for both two-dimensional and three-dimensional approaches: the static droplet and the oscillating droplet. Finally, to verify the applicability of the methodology to flows involving topological changes, two-dimensional coalescence cases of two initially circular bubbles and of two Taylor bubbles were simulated. The results obtained for the referred simulations showed a substantial compatibility with analytical solutions and experiments reported in the literature, corroborating the validity of the methodology for the description of two-phase flows.

3.1 Static Droplet

This test consists in simulating a circular/spherical droplet of fluid in a quiescent medium. This evaluates the equilibrium between the pressure and the surface tension force, and it is a measure of the method's stability. At the upper boundary of the domain, a condition of prescribed zero pressure was imposed, while at the other boundaries, no-slip conditions were imposed.

For the simulation of the two-dimensional case, a circular droplet with diameter $D = 1$ is considered, immersed in a square domain with side length $L = 4$. The simulation was carried out with $We = 10$, $Re = 100$, and the following properties: $\rho_{in} = 0.01$ and $\mu_{in} = 0.5$ for the internal fluid, and $\rho_{out} = 1$ and $\mu_{out} = 1$ for the external fluid. Two triangular meshes were used: one mesh with 47566 mini elements and 71618 nodes; and one mesh with 47566 quadratic elements and 95669 nodes. For the representation of the droplet, initially, a mesh with 112 points was defined in order to match the refinement of the interface with that of the static mesh. The flow was simulated for 1000 iterations, with a time step of $\Delta t = 0.005$. A comparison between the horizontal pressure profiles passing through the center of the droplet obtained in the simulations and the analytical profile, characterized by a uniform pressure inside the droplet with a value of 0.2, is shown in Figure 1. For both mini and quadratic elements, the final obtained internal pressure was 0.200079, resulting in an error of 0.039%, highlighting the high compatibility between the applied methodology and theory.

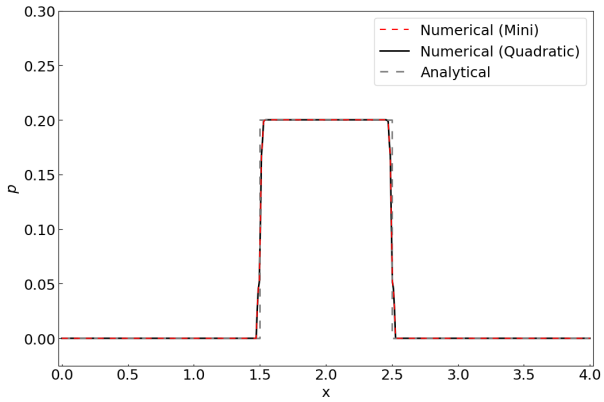

Figure 1. Comparison between the horizontal pressure profile obtained at the end of the simulation and the analytical profile for the static droplet two-dimmensional simulation.

For the three-dimensional case, the simulation was executed with the following parameters: $Re = 1, We = 1$, $\rho_{in} = 1$, $\mu_{in} = 1$, $\rho_{out} = 0.001$ and $\mu_{out} = 0.001$. A tetrahedral mesh with 110464 mini elements and 131888 nodes was used to discretize a domain with side length $L = 2$. The flow was simulated for 1000 iterations, with a time step of $\Delta t = 0.005$. A study regarding the intensity of the spurious velocities and the pressure error was conducted, and its results are shown in Table 1. The simulation appears to degrade when the interface mesh average edge length is smaller than the fluid mesh average edge length; optimal values are obtained with closely matched average edge lengths.

Table 1. Spurious velocity intensity and pressure error for the three-dimensional static droplet test case.

Number of nodes	v_{max}	Δp_{error}
159	6×10^{-1}	0.408%
317	1.9×10^{-2}	0.118%
625	1.2×10^{-2}	0.102%
1141	4×10^{-3}	0.061%
4308	4.2×10^{-1}	18.4%
9500	366	1223.1%

3.2 Oscillating Droplet

The problem of the oscillating droplet is quite similar to that of the static droplet. In this case, a initially stationary droplet immersed in another fluid without the action of gravity is also considered, and the same boundary conditions are imposed. However, an initial perturbation in the droplet diameter is considered, characterizing an elliptical/ellipsoidal geometry. It is expected that the interfacial tension leads to a reduction in the eccentricity of the droplet, which, combined with the damping caused by viscosity, will cause a damped harmonic oscillator motion. The frequency of this oscillation can be calculated analytically through the theory developed by Strutt [12] and extended by Fyfe et al. [13], represented by (9), where n is the mode of oscillation, σ is the interfacial tension, ρ_{in} is the density of the droplet fluid, ρ_{out} is the density of the external fluid, and R is the reference radius of the droplet.

$$\omega = \sqrt{\frac{(n^3 - n)\,\sigma}{(\rho_{in} + \rho_{out})\,R^3}} \tag{9}$$

For the two-dimensional case, this flow was simulated with a droplet of diameter $D = 1$, with an initial horizontal perturbation of 0.01. The defined parameters for the flow were $Re = 100$, $We = 10$, $\rho_{in} = 1$, $\mu_{in} = 1$, $\rho_{out} = 0.001$ and $\mu_{out} = 0.01$, and the same meshes from the static droplet simulation were used. The flow was simulated for 1600 iterations, with a time step of $\Delta t = 0.005$. Using these parameters, the analytical oscillation frequency $\omega = 2.1898$ was calculated through (9) for the lowest oscillation mode ($n = 2$). The simulations with mini and quadratic elements resulted in frequencies of 2.1542 and 2.1543, respectively, leading to relative errors of -1.63% and -1.62%. For the three-dimensional case, the flow was simulated with $Re = 500$, $We = 80$, $\rho_{in} = 1$, $\mu_{in} = 1$, $\rho_{out} = 10^{-6}$ and $\mu_{out} = 10^{-6}$. A fluid mesh with 210724 nodes and an interface mesh with 898 nodes were used. The simulation was conducted over 600 iterations with a time step of $dt = 0.02$. The analytical frequency is 0.8944, and a frequency of 0.9372 was obtained from the simulation, leading to a relative error of 4.78%. For both cases, the evolution of the droplet's horizontal length over time is shown in Figure 2.

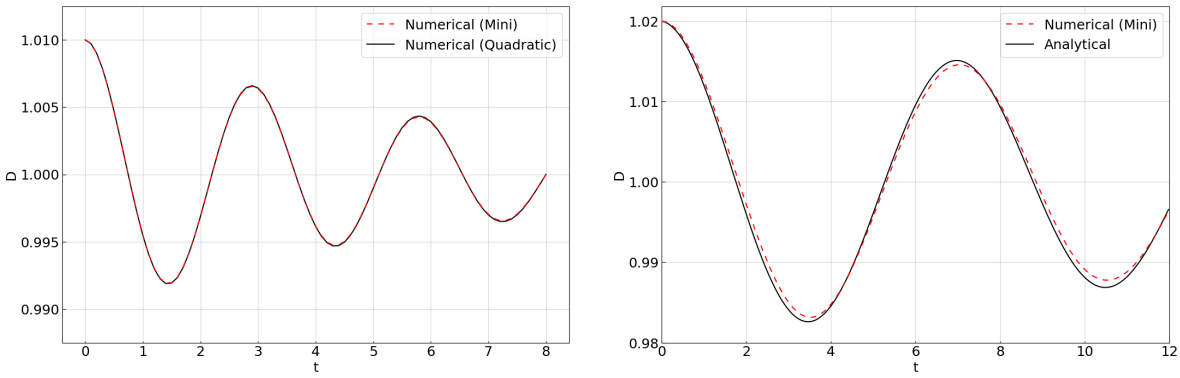

Figure 2. Evolution of the horizontal length of the oscillating droplet during the two-dimmensional (left figure) and the three-dimmensional (right figure) simulations.

3.3 Two-dimmensional coalescence of Two Rising Bubbles

This simulation involves the flow of two bubbles rising under the influence of gravity, and the coalescence phenomenon is observed, following the methodology described in the previous section. The initial geometry of the flow consists in two bubbles with diameter $D = 1$, whose centers are separated by a distance of 1.18, in a rectangular domain with width equal to 5 and height equal to 10. There were imposed a no-slip boundary condition at the bottom boundary of the domain, symmetry conditions at the left and right boundaries and a prescribed zero pressure condition at the upper boundary.

The simulation parameters were inspired by an air-glycerine system experiment conducted by Manasseh et al. [14]: $Ga^{1/2} = 10$, $Eo = 5$, $\rho_{in} = 1.44$, $\mu_{in} = 0.01$, $\rho_{out} = 1220$ and $\mu_{out} = 1$. Two triangular meshes were used: one mesh with 33204 mini elements and 50046 nodes; and one mesh with 33204 quadratic elements and 66687 nodes. For the representation of the bubbles, initial meshes with 50 points were defined to match their refinement with that of the static mesh. The flow was simulated for 46000 iterations, with a time step of $\Delta t = 0.0001$. The validation of the methodology was performed by comparing the simulations interface geometry with those of the experiment conducted by Manasseh et al. [14], as shown in Figure 3.

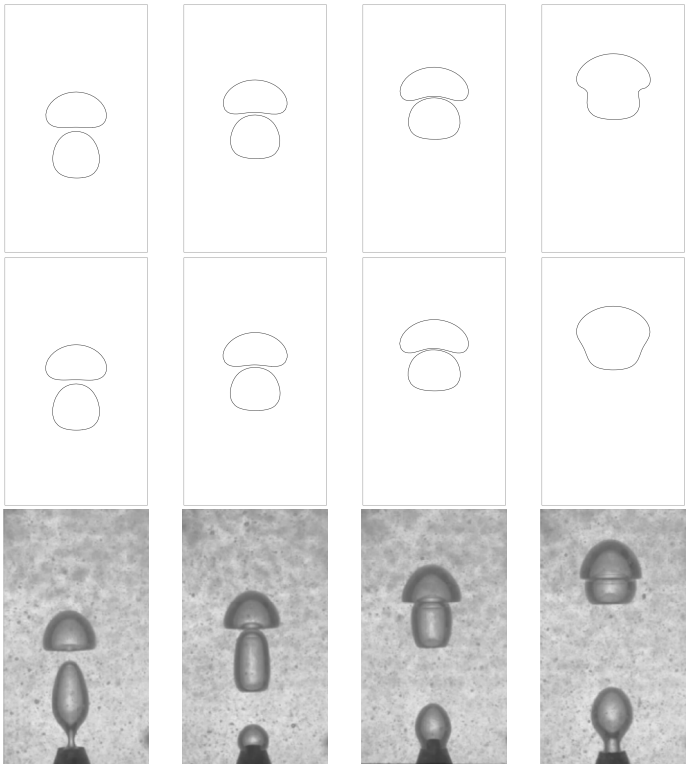

Figure 3. Interface geometry at instants $t = 2.0$, $t = 2.5$, $t = 3.0$, and $t = 3.5$ for the simulation with the mini elements mesh (top row), the simulation with the quadratic elements mesh (middle row) and the experiment of coalescence of two bubbles conducted by Manasseh et al. [14] (bottom row).

Coalescence simulation of Taylor bubbles have also shown good agreement with its expected behavior, as depicted by Figure 4, with the recently coalesced Taylor bubble achieving its characteristic shape after a damped wave propagation on the interface. The flow initial geometry consists in two elliptical bubbles with horizontal semi-axis of 0.48 and vertical semi-axis of 0.88, making them equivalent in area to a circular bubble with a diameter 30% larger than the channel width $L = 1$. The channel has a height of 10, and the bubbles are initially separated by a distance of 0.25. The flow was simulated with the parameters $Ga^{1/2} = 10$ and $Eo = 5$, and for the fluids, based on an air-water system, the following properties were considered: $\rho_{in} = 1.145$, $\mu_{in} = 1.79 \times 10^{-5}$, $\rho_{out} = 997$ and $\mu_{out} = 89 \times 10^{-5}$. A mesh with 18952 quadratic elements and 38493 nodes was used. For the representation of the bubbles, initial meshes with 115 points were defined to match their refinement with that of the static mesh. The flow was simulated for 9000 iterations, with a time step of $\Delta t = 0.0025$. Even with more critical conditions involving wall effects on bubble dynamics, it is observed that the proposed methodology was able to describe both the flow and the coalescence phenomenon in a feasible manner, confirming the expected behaviors based on the physics of the problem.

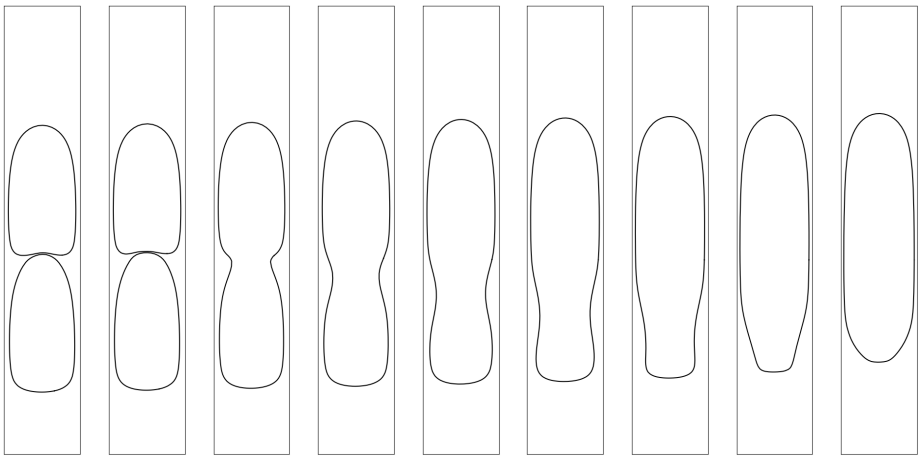

Figure 4. Evolution of the interface geometry in the coalescence of two Taylor bubbles simulation.

4 Conclusion

In this work, a methodology is presented for the study of two-phase flows using direct numerical simulation, based on the two-dimensional incompressible Navier-Stokes equations, the Finite Element Method, the semi-Lagrangian method, and an interface-tracking strategy. In summary, the variety of simulated flows allowed us to confront the proposed methodology from different perspectives, and the accuracy of the results for the various analyzed phenomena corroborated its validity in describing them. Therefore, it is demonstrated that the new method proposed in this work is accurate for simulating two-dimensional and three-dimensional two-phase flows, with the presence of confined droplets and bubbles and the occurrence of topology changes. Ongoing and future efforts are focused on the development of adaptive refinement for both domain and interface meshes, as well as on the implementation of three-dimensional models for bubble coalescence and break-up.

Acknowledgements. The research leading to these results received funding from the Brazilian Higher Education Agency (CAPES), the Research Support Foundation of the State of Rio de Janeiro (FAPERJ) and by the Royal Society-Newton Advanced Fellowship [NAF\R2\202165] as part of the Newton Fund in partner-ship with CONFAP and CNPq.

Authorship statement. The authors hereby confirm that they are the sole liable persons responsible for the authorship of this work, and that all material that has been herein included as part of the present paper is either the property (and authorship) of the authors, or has the permission of the owners to be included here.

References

[1] G. Tryggvason, R. Scardovelli, and S. Zaleski. Direct numerical simulations of gas–liquid multiphase flows. *Cambridge University Press*, 2011.
[2] A. Wiin-Nielsen. On the application of trajectory methods in numerical forecasting. *Tellus*, vol. 11, n. 2, pp. 180–196, 1959.
[3] J. S. Sawyer. A semi-lagrangian method of solving the vorticity advection equation. *Tellus*, vol. 15, n. 4, pp. 336–342, 1963.
[4] Y. Maday, A. T. Patera, and E. M. Rønquist. An operator-integration-factor splitting method for time-dependent problems: Application to incompressible fluid flow. *Journal of Scientific Computing*, vol. 5, pp. 263–292, 1990.
[5] K. Boukir, Y. Maday, and B. Métivet. A high order characteristics method for the incompressible navier—stokes equations. *Computer Methods in Applied Mechanics and Engineering*, vol. 116, n. 1, pp. 211–218, 1994.
[6] R. Phillips and T. Phillips. Flow past a cylinder using a semi-lagrangian spectral element method. *Applied Numerical Mathematics*, vol. 33, n. 1, pp. 251–257, 2000.
[7] E. Celledoni, B. K. Kometa, and O. Verdier. High order semi-lagrangian methods for the incompressible navier–stokes equations. *Journal of Scientific Computing*, vol. 66, n. 1, pp. 91–115, 2015.
[8] D. Wilde, A. Krämer, D. Reith, and H. Foysi. High-order semi-lagrangian kinetic scheme for compressible turbulence. *Phys. Rev. E*, vol. 104, 2021.
[9] G. Anjos, G. Oliveira, N. Mangiavacchi, and J. Thome. One- and two-step semi-lagrangian integrators for ale-fe two-phase flow simulations. *International Journal for Numerical Methods in Fluids*, vol. 94, 2022.
[10] M. Sussman and P. Smereka. Axisymmetric free boundary problems. *Journal of Fluid Mechanics*, vol. 341, pp. 269–294, 1997.
[11] S. O. Unverdi and G. Tryggvason. A front-tracking method for viscous, incompressible, multi-fluid flows. *Journal of Computational Physics*, vol. 100, n. 1, pp. 25–37, 1992.
[12] J. W. Strutt. Vi. on the capillary phenomena of jets. *Proceedings of the Royal Society of London*, vol. 29, n. 196-199, pp. 71–97, 1879.
[13] D. Fyfe, E. Oran, and M. Fritts. Surface tension and viscosity with lagrangian hydrodynamics on a triangular mesh. *Journal of Computational Physics*, vol. 76, n. 2, pp. 349–384, 1988.
[14] R. Manasseh, S. Yoshida, and M. J. Rudman. Bubble formation processes and bubble acoustic signals. *Third International Conference on Multiphase Flow (ICMF'98)*, 1998.